Proceedings of the Pakistan Academy of Sciences 51 (1): 67–81 (2014)

ISSN: 0377 - 2969 (print), 2306 - 1448 (online)

Pakistan Academy of Sciences

Research Article

Computation and Modeling of the Variability in Electron Concentration and Refractive Index for F_2 Layer at Pakistan Region

Syed Nazeer Alam[1*], Muhammad Ayub Khan Yousuf Zai[2] and Akbar Ali Jilani[3]

[1]Department of Electronics & Power Engineering, Pakistan Navy Engineering College, National University of Sciences & Technology, Karachi, Pakistan
[2]Department of Applied Physics, Solar-Terrestrial & Atmospheric Research Wing and Institute of Space & Planetary Astrophysics, University of Karachi, Karachi, Pakistan
[3]Solar-Terrestrial & Atmospheric Research Wing and Institute of Space & Planetary Astrophysics, University of Karachi, Karachi, Pakistan

Abstract: The ionosphere is electrically conducting region of the upper atmosphere, plays an important role in the ionospheric region on electromagnetic waves of 3 MHz to 30 MHz transmitted from ground station to reach to a receiving station. The low-frequency is limited by signals reflected from ionosphere and other range of frequencies are refracted from ionosphere layers depending upon time, height, season, temporal variations due to solar radiations, Sunspots and Earth magnetic field variations. In this communication the F_2 layer data recorded at SUPARCO Islamabad Ionosphere Station (SIIS) for the year 2005 has been used to compute useful ionosphere parameters in respect of ordinary critical frequency (3.04 to 8.29 MHz) at different altitudes of ionosphere with variation in ion composition of F_2 layer. The geographic location of SIIS is latitude 33.75°N and longitude 72.87°E. The critical frequency and height recorded on hourly basis have been used to compute the ionosphere parameters such as electron concentration and refractive index. The temporal estimation of parametric variability is determined, for estimation and modeling purposes standard statistical techniques have been preferred for regression and autocorrelation according to suitability of data trend/pattern. The aspect of study is useful in predicting and forecasting for sky wave communication. The result derived from study is useful for public, governmental and private sector organizations dealing with the business of radio wave communication in the region of Pakistan.

Keywords: Ionosphere, critical frequency, electron density, temporal variations, sunspot

1. INTRODUCTION

The ionosphere extends in the height from 70 to 600 Km above the sea level. Ionospheric regions are conventionally designated as $\mathrm{C, D, E}$ and F. Each region is characterized by degree of ionization that dependent on strength of solar radiations. The most important ionizing agents are ultraviolet and Alpha and Gama radiation from the Sun, as well as cosmic rays and meteors. The $\mathrm{D, E}$ and F layers show electron density peaks. The ionization is the greatest in the summer and day time, least in the winter and night. The Sunspot, a standard index of solar activity has influence on the radio flux density of ionosphere [1]. The ionosphere tends to be stratified, rather than regular, in its distribution. The existence of ionosphere as an electronically conducting region

Received, April 2012; Accepted, December 2013
*Corresponding author: Syed Nazeer Alam; email: nazeer@pnec.nust.edu.pk

had been postulated earlier in 1883 to explain the daily variations in the geomagnetic field in 1902 correctly surmised that ionosphere contains free electrons and ions produced by solar ionizing radiation [3]. Research began in 1924 when Appleton and Barnett and Breit and Tuve measured the height of the ionosphere reflecting layers. From 1972 to 1975 NASA launched the AEROS and AEROS B satellites to study the F region [2]. The ionosphere is a region having refractive index < unity computed in terms of critical frequency and EM wave incident angle. In this study ground base recorded ionosphere data of year 2005 over Pakistan, Islamabad region is used to compute more important parameters which helped in establishing and presenting, sampling distribution, regression, correlation and modeling of recorded and investigated parameters.

2. THE F_2 LAYER

The computation of ionosphere electron concentration (N) resulted in varying refractive index (n) of F_2 layer and its effect on the long distance communication has been presented in the study. Any vertically launched waves can be reflected and oblique waves are progressively bent away from the vertical. The F layer extends 100 Km to 300 Km above the earth's surface. This layer is maintained during day and night. During the daytime, the F region is bifurcated into F_1 and F_2 layers. The F_1 layer is the region extending at altitudes ranging from 150 Km to 210 Km which presents a regular stratification at moderate latitudes. The total electron concentration (TEC) in F_2 layer is greater than F_1 layer because of smaller electron loss. The electronic concentration in this layer vary $5 * 10^{11}$ electron/m^2 during the night and $20 * 10^{11}$ e/m^{2}during the day and is heavily influenced by a) neutral winds, b) diffusion, c) by different other dynamic effects [2].

3. METHODOLOGY

The ionosphere, act as reflectors or absorbers to radio waves at frequencies below about 30 MHz The following methodology to compute important ionosphere parameters, develop model, to apply statistical analysis such as regression, correlation, time series to investigate data seasonality/trends of the recorded and investigated parameters have been presented in this study with conclusion at the end. The computation and modeling of electron density and refraction index from the known recorded data for the (April-Dec) year 2005 over Pakistan ionosphere region is the main objective of this study. To understand parametric variability and its relationship the following valid mathematical tools have been used.

3.1 Electron Density and Critical Frequency

The density of electrons in the ionosphere also varies as a function of geomagnetic latitude, diurnal cycle, yearly cycle, and sunspot cycle. The reflection from the F_2 layer is the major factor in HF communications. The critical frequency is the limiting frequency at or below which a radio wave is reflected by an ionosphere layer at vertical incidence. The highest frequency returned to earth when radiated upward in the vertical direction. Its value is dependent on the composition of ionosphere i.e. strength of the electron concentration. For F_2 layer the ordinary critical frequency (f_c) is related to peak value of (N) given in Eq-(1). The ionosphere conditions change from hour to hour, day to day, month to month, season to season and year to year therefore, the f_c also changes constantly. The recorded hourly maximum and minimum critical frequency is 8.28 MHz and 3.03 MHz respectively. The peak value of electron density of F_2 layer is calculated in respect of measured ordinary critical frequency, the expression in Eq-(2) postulated by Anderson and Matsushita [1&3] in 1974.

$$f_c = \sqrt{80.8}N \cong 9\sqrt{N(max)} \tag{1}$$

$$N(max) = 1.24 * 10^4 f_c{}^2 (MHz) \quad e/cm^3 \tag{2}$$

The computed electron concentration maximum value $8.5166*10^{11}$and minimum value are $1.1441*10^{11}$ with mean of $3.1829*10^{11}$ having standard deviation of $9.9092*10^{10}$ electron/cm^3. For the F_2 layer the extraordinary critical frequencies, which exist because of the birefringence caused by the Earth's magnetic field is determined using extra ordinary critical frequency (f_x) is determined using gyro-frequency (f_g) given in Eq-(3). The gyro-frequency of a charged particle is its rate of gyration in a magnetic field. If the magnetic induction (B) is gradually increased, the gyration frequency is increased in proportion. For a magnetic field (B) of 0.5 gauss ($0.5 * 10^{-4}$ Wb/m^2) the gyro-frequency for Islamabad region is calculated [4]. The electron count in respect of extra-ordinary critical frequency is calculated with the help of Eq-(4).

$$f_g = \frac{B\,q}{2\pi m} \equiv 1.4 \quad \text{MHz}$$

$$f_x = f_o + \frac{f_g}{2} \quad \text{MHz} \tag{3}$$

$$Nx(max) = 1.24 * 10^4 ({f_x}^2) \quad e/cm^3 \tag{4}$$

3.2 Refraction in Ionosphere

The ionosphere is weak plasma. A vertically launched waves can be reflected and an oblique waves are progressively bent away from the vertical. The amount of refraction depends on three main factors: (a) the density of ionization of the layer, (b) the frequency of the radio wave, and (c) the angle at which the wave enters the layer. The dielectric approach for ionosphere as proposed by Larmor in 1924 is appropriate for most radio frequencies; the absorption is relatively small inside the ionosphere, and the wave is returned the ground by gradual refraction [4]. Total refraction occurs when the collision frequency of the ionosphere is less than the radio frequency and if the electron density in the ionosphere is great enough. The velocity of an electromagnetic wave in vacuum is equal to velocity of light but in ionosphere medium it is given by $v = \frac{c}{n}$, where n is refractive index of ionosphere medium rather than property of wave. In the simplified form refractive index mentioned in Eq. (5) of ionosphere is given by Appleton-Hartee expression [1, 5].

$$n^2 = 1 - \frac{X(1-X)}{(1-X) - \frac{1}{2}Y_T^2 \pm [\frac{1}{4}Y_T^4 + (1-X)^2 Y_L^2]^{\frac{1}{2}}} \tag{5}$$

where,

$$X = \frac{N\,e^2}{\varepsilon_0 m\omega\text{^}2}\ , \quad Y_L = \frac{e\,B_L}{m\omega} \text{ and } Y_T = \frac{e\,B_T}{m\omega}$$

If θ is the angle between the propagation direction and the geomagnetic field, then $\omega_L = \omega_g \cos\theta$ and $\omega_T = \omega_g \sin\theta$.In the simplest case, when there are no collisions (Z = 0) and the magnetic field is neglected ($Y_L = Y_T = 0$) the Eq-(5) becomes [4];

$$n^2 = 1 - X = 1 - \omega_N^2 / \omega^2$$

$$= 1 - Ne^2 / \varepsilon_0 m\omega^2 \tag{6}$$

If the magnetic field is included the refractive index becomes double valued. The two waves are called the characteristic waves, the upper sign giving the so-called ordinary wave, and the lower sign the extraordinary wave. When collisions are significant ($Z \neq 0$) the refractive index is complex. The ionosphere is a nonmagnetic medium the expression (7) expresses the dielectric constant (k):

$$n^2 = c^2 / v^2 = \mu_0\, \varepsilon / \mu_0 \text{ and } \varepsilon_0 = \varepsilon / \varepsilon_0 = k \tag{7}$$

In our case the variation in the computed values of refractive index is 0.9525 to 0.9485 with mean 0.9502 and a least standard deviation of 0.0005 subject to bending of EM wave in F_2 and F layers which finally helps in establishing long distance communication. It is the angle above which the signal will not be reflected enough to return to earth. It has been observed that by lowering the radiation angle from the exact vertical direction allows the wave to travel longer through the ionosphere layers. It is also seen that signals above the critical angle penetrate the ionosphere layers while below this angle the wave returns to earth. The critical angle for radio waves depends on the layer electron density and the wave length of the signal. As the frequency of a radio wave is increased, the critical angle must be reduced for refraction to occur. The critical frequency which is proportional to:

$$f_{muf} = f_c \text{ Sec i} \tag{8}$$

4. EXPLORATORY DATA ANALYSIS

In this study hourly monthly-median values of the critical frequency of the daytime F_2 layer and the night-time F region, measured at mid-latitude at Islamabad region are used. The exploratory data analysis is an important part of statistical analysis. EDA approach relies heavily on graphical techniques i.e. plotting of histogram for representation of distribution with single quantitative variable. The continuous envelope provides the hypothetical limit of samples. In this particular study, the sampling distribution of critical frequency, electron concentration and refractive index is witnessed in histogram plots shown in Figs. 1 to 3. The distributions are symmetrical and tend to show Gaussian normal distribution for sample value S= 153. The variability in ionosphere chemistry due to change in solar radiation, (N) is subject to change in (n) and to put impact on the long distance communication at Pakistan region has been investigated and presented.

4.1 Regression Analysis

It has been observed that the correlation between the parameters can be evaluated using scatter plots which are useful diagnostic tool for investigating association between two variables. The bivariate distribution presented in scatter plot shown in Fig. 4 display fairly high degree of positive correlation between ordinary critical frequency (recorded by DG 256 Ionosphere Receiver installed at SUPARCO Ionosphere Station at Islamabad) and electron concentration of F_2 layer. Scatter plots are useful diagnostic tool to investigate association between two variables. The bivariate distribution presented in scatter plot shown in Fig. 4 display fairly high degree of positive correlation between ordinary critical frequency and electron concentration of F_2 layer, a straight line having intercept equals to $-3.5777 * 10^{11}$ and slope of line = $1.3484*10^{11}$ show comfortably fits through our sample data consisting of 153 observations. The Pearson's statistic, r = 0.9925 is very close to unity. This shows strong relationship i.e. changes in one variable with changes in the second variables [6]. The regression fit equation is;

$$N = -3.5777 * 10^{11} + 1.3484 * 10^{11} f_c \tag{9}$$

The relationship between refractive index and critical frequency show a strong negative correlation, r = − 0.9739 with two outliers, a straight line with intercept of 0.9537 and slope equals to - 0.0007, witnessed comfortably fits through the computed data values. This is translated as for decreasing values of refractive index the critical frequency increased as shown in Fig. 5. The regression line equation is;

$$n = 0.9537 - 0.0007 f_c \tag{10}$$

The regression between (N) and (n) is an approximate linear relationship but it reveals a negative correlation statistical condition, r = -0.9399 referred to as hetero-scedasticity i.e. non-constant variation in data points. The presence of outliers is due to either measurement error or recording equipment malfunctioning. The regression line equation is;

$$n = 0.9518 - 5.0118*10^{-15} N \tag{11}$$

The coefficient of correlation (r), measure of the closeness of a fit in the relative sense, coefficient of determinant (r^2) tells the process of variation of the parameters. The error (P) and for significant correlation covariance < 6 (coefficient of correlation). The Pearson's correlation values in each case are mentioned in the Table 1.

Table 1. Correlation statistics**.**

Parameter	r	r^2	P
N Vs f_c	0.9925	0.9850	0.0000
n Vs f_c	- 0.9725	0.9485	0.0000
n Vs N	- 0.9399	0.8834	0.0000

4.2 Normal Probability Plot

Diurnal daily and monthly distributions of ion concentration are presented and the relative role of the solar radiation has been evaluated. The normal probability plot is a special case of the probability plot. The points that fall on the fitted straight line indicate a normal distribution. The Fig. 7 form a nearly linear pattern indicates that the normal distribution is a good model for the refractive index. Departures from the straight line indicate

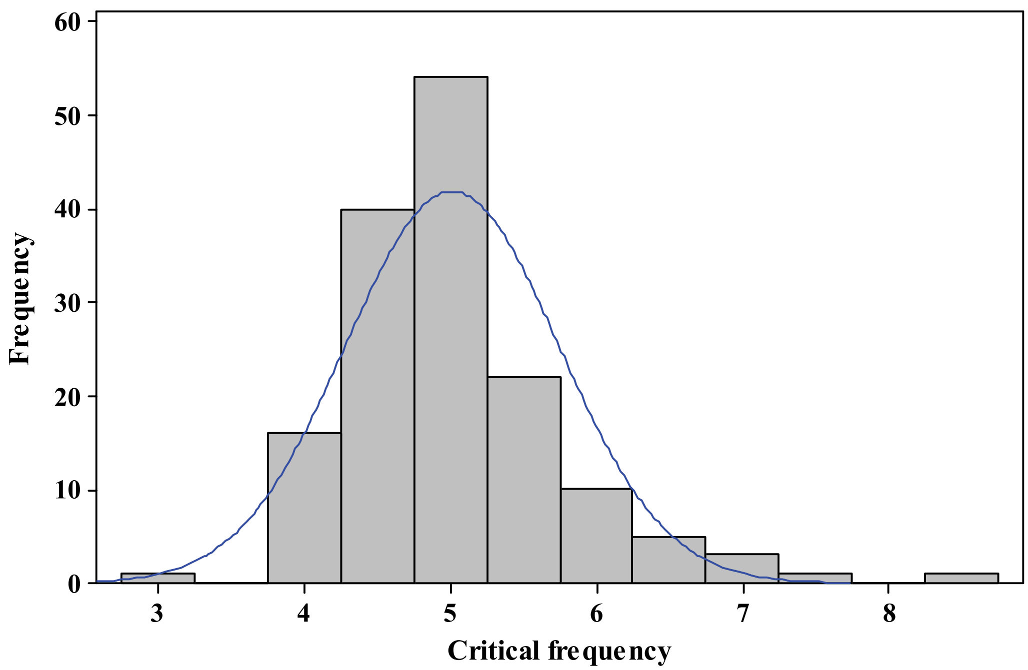

Fig. 1. Histogram of observed critical frequency with normal curve.

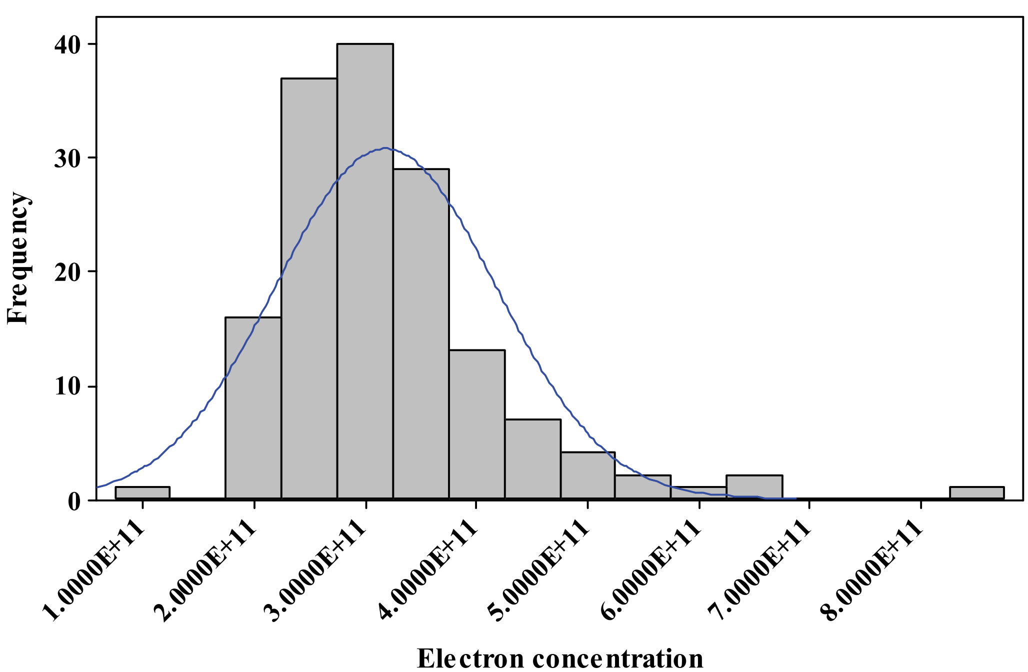

Fig. 2. Histogram of observed electron concentration with normal curve.

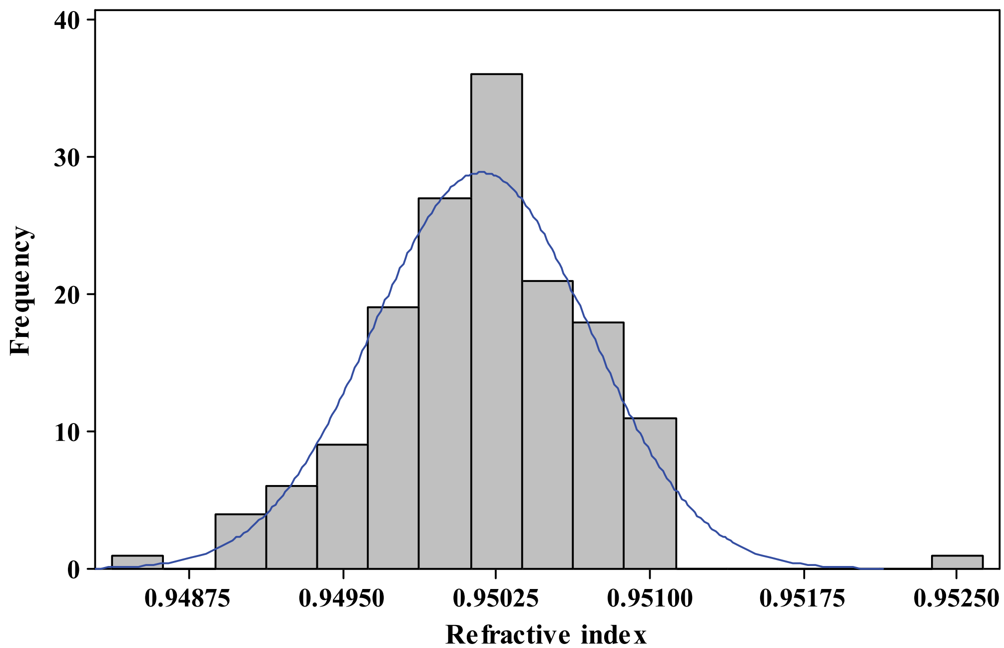

Fig. 3. Histogram of observed refractive index with normal curve.

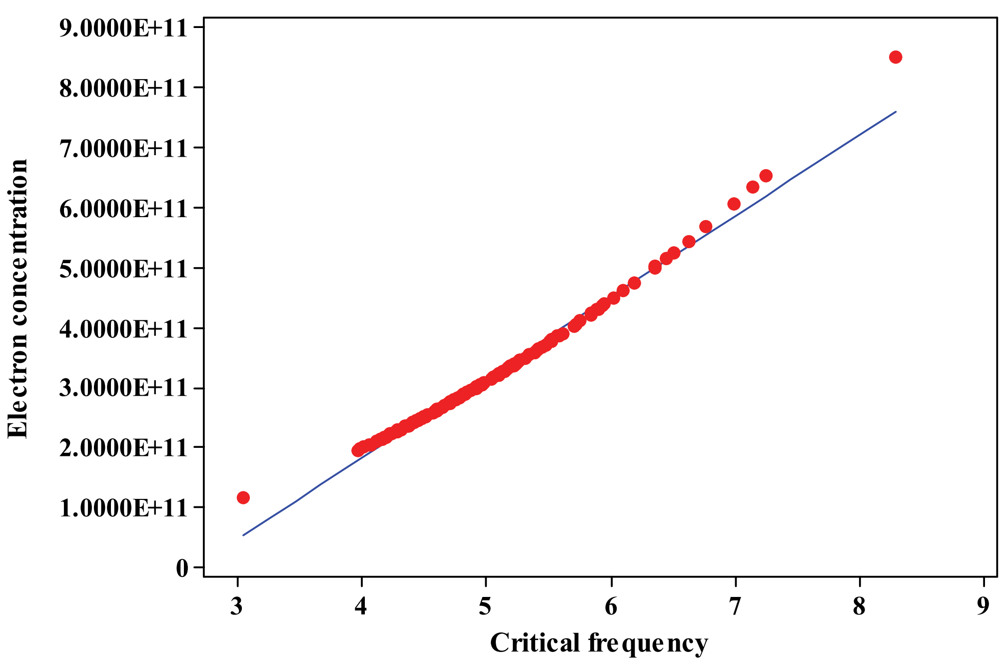

Fig. 4. Scatter pot of electron concentration and critical frequency.

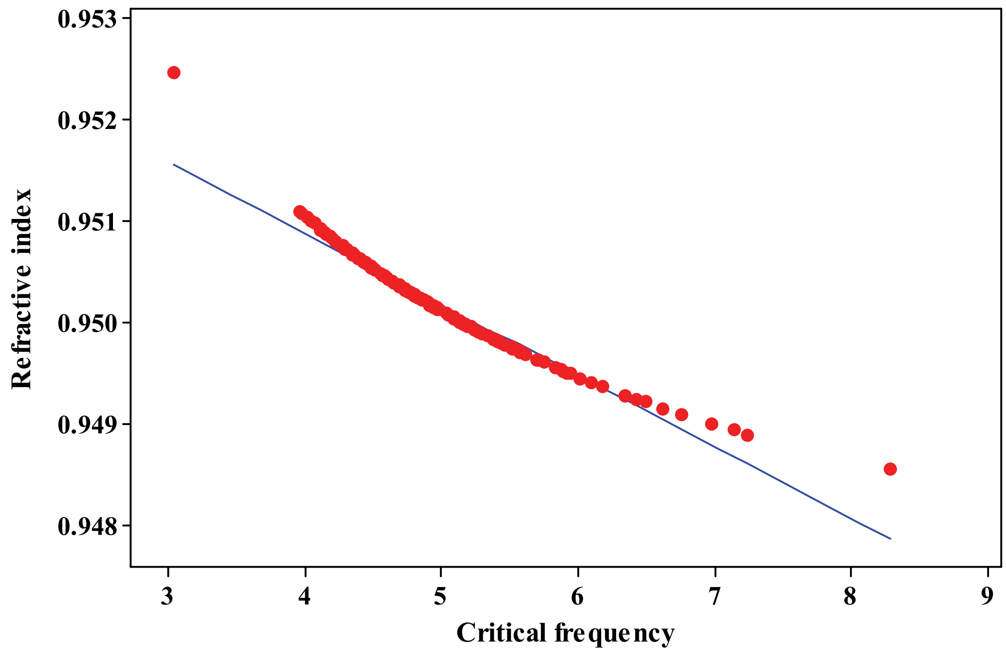

Fig. 5. Scatter pot of refractive index and critical frequency**.**

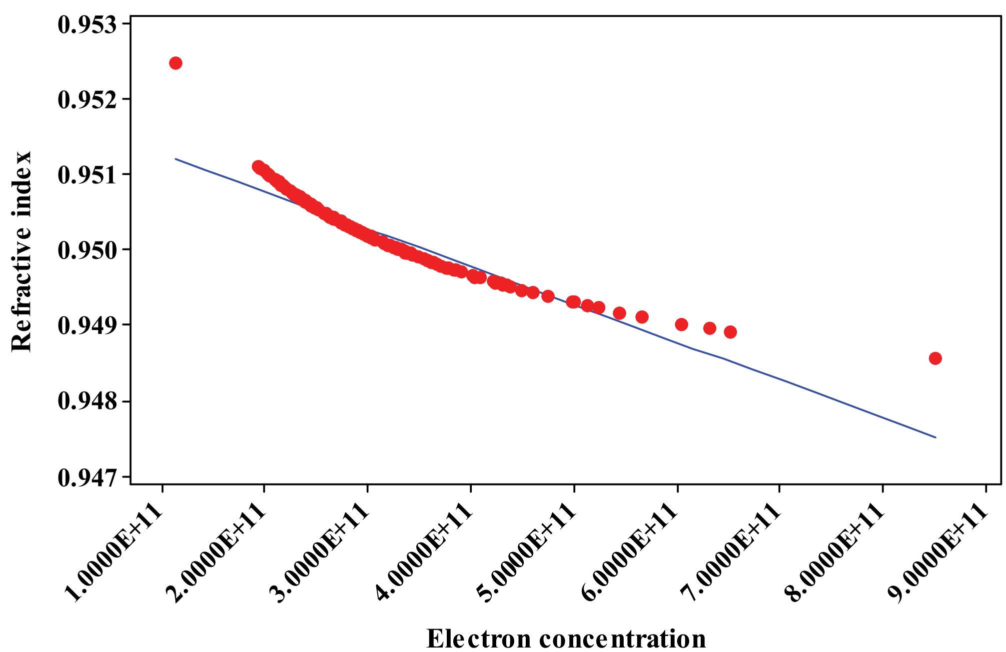

Fig. 6. Regression between refractive index and electron concentration.

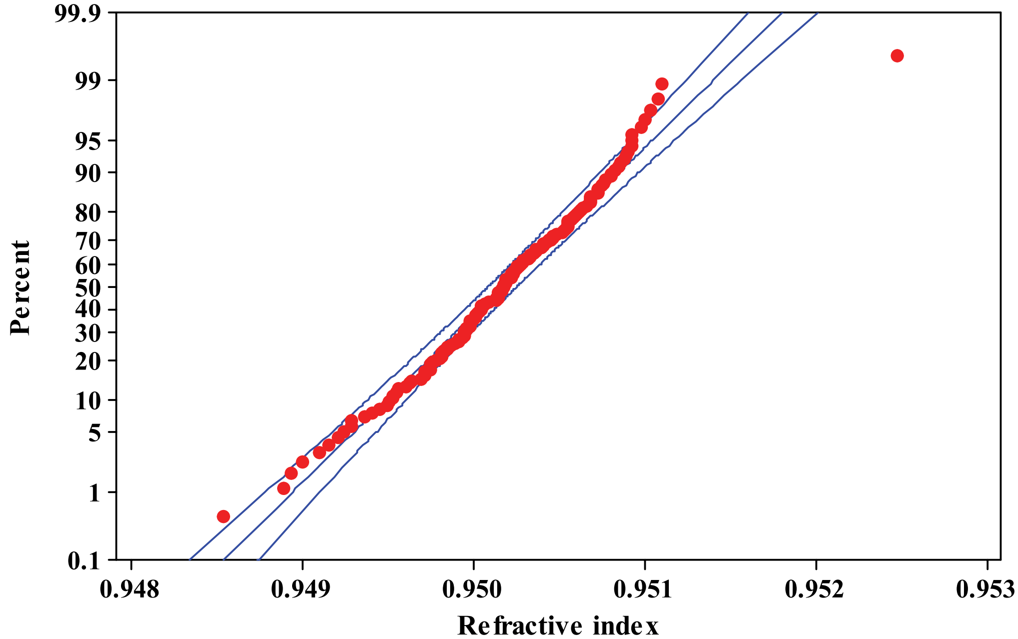

Fig. 7. Normal probability plot of refractive index.

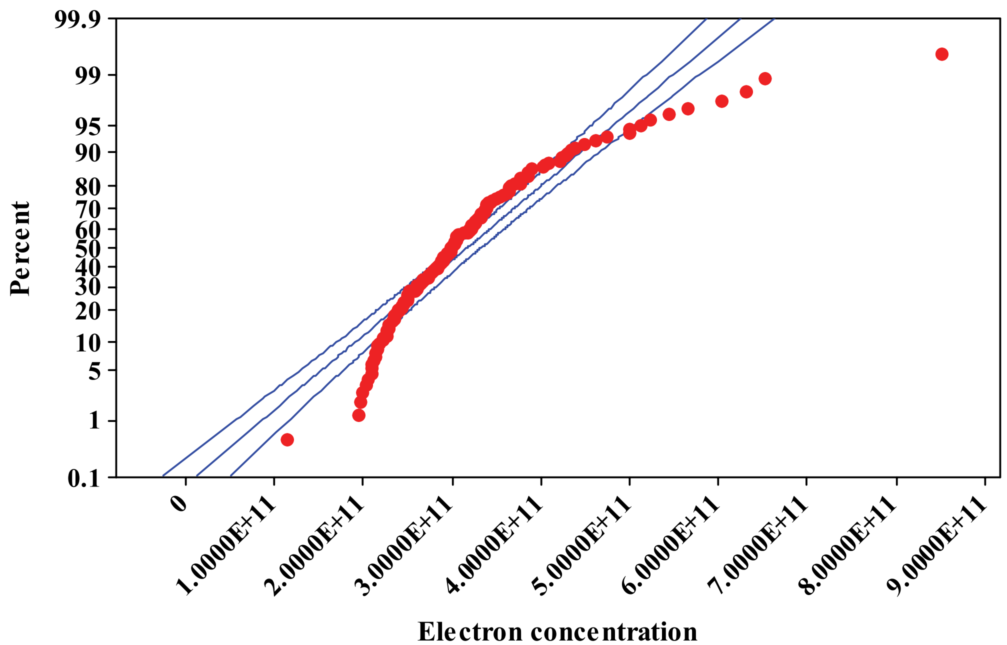

Fig. 8. Normal probability plot of electron concentration.

departures from normality. In Fig. 8: the fitted line indicates departure of data from extremes. It is evident that the data do not follow normal distribution. A convex curve illustrate that the distribution is skewed to the left [7].

4.3 Inferential Aspects

Time series data have a natural temporal ordering. The time domain approach of time series analysis suggests correlation between adjacent points in time is best investigated in terms of a dependence of the current value on the past values. It also focuses on modeling some future value of a time series as parametric function of the current and previous values [8]. In this communication seasonal pattern with periodic behavior of variation in electron concentration and refractive index against time is shown in Figs. 9 and 10, show variations reflecting increase and decrease of data in the ionosphere of F_2 layer in day time and F during night over Pakistan region.

4.4 Smoothing

Smoothing data removes random variation and shows trends and cyclic components. This technique, when properly applied, reveals more clearly the underlying trend, seasonal and cyclic components. Non-stationarity present in time series plots are removed by differencing the data or by fitting some type of trend curve. The time series plots indicate a falling trend for electron concentration and a rising trend for refractive index under discussion. A visual inspection of these plots indicates that a simple linear fit is sufficient to remove the trend but the variance (amplitude) is still varying with time. The residual plots along with actual time series and smoothed series for fitting with linear trend curve for both parameters is shown separately [8]. The single exponential smoothing assigns exponentially deceasing weights over for TEC and refractive index is for known sample values are represented in mathematical form in terms of forecast in equation. The smoothing coefficient (α) explains degree of smoothing and how responsive the model is to fluctuation in the time series data of reported parameters.

$$F_{t+1} = \alpha\, Y_t + (1-\alpha)\, F_t \qquad (12)$$

$$0 < \alpha \le 1 \quad t > 0$$

The single exponential smoothing of TEC is computed with α = 0.3 for minimum mean % error (MPE) and mean absolute % error (MAPE) with least residual show a fairly stable model as shown in Fig. 11.

Table 2. The summary of error.

Summary of Error	Error for TEC	Error for Refractive Index
Mean Error	$1.341677*10^{9}$	- 0.000012
Mean Absolute Error	$5.057756*10^{10}$	0.000029191
Sum of Squares	$9.383986*10^{23}$	0.0000247
Mean Squares	$6.133324*10^{21}$	0.0000
Mean % Error	- 2.847449	- 0.0012796
Mean Absolute % Error	$1.574324*10^{1}$	0.0307216

The smoothing of Refractive Index is computed with α = 0.25 for minimum mean % error (MPE) and mean absolute % error (MAPE) with least residual as shown in Fig. 12. The summary of errors for both parameters is mentioned in Table 2. The residual analysis determined by single exponential smoothing shows a sufficiently high degree of correlation and a stable model. The Bootstrapping forecast technique explained in Eq-(12) is used to forecast the parameter under study. The forecast values with single exponential smoothing for TEC and refractive index are computed in Eqs-(14) & (15) respectively using model Eq- (13).

$$F_{t+1} = F_t + \alpha\,(X_t - F_t) = F_t + \alpha\,(e_t) \qquad (13)$$

$$F_{154} = (0.3)\, Y_{153} + (0.7) F_{153} = 2.88873*10^{11} \qquad (14)$$

$$F_{154} = (0.25)\, Y_{153} + (0.75)\, F_{153} = 0.950378 \qquad (15)$$

4.5 Model Strategies

There are many methods used to model and forecast time series. The most commonly used model fitting include Box-Jenkins (1976-1996)

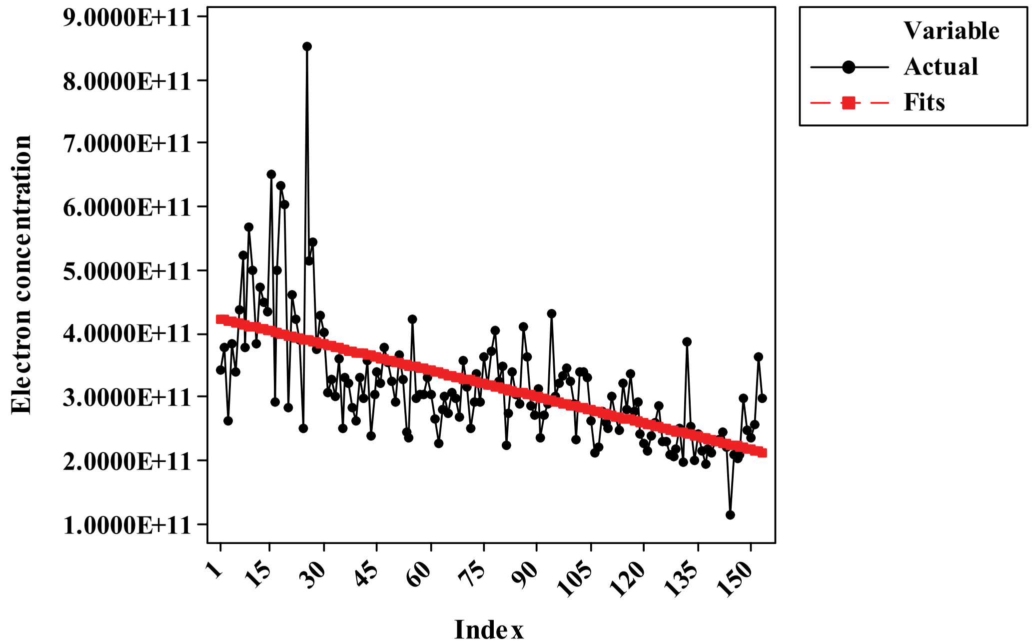

Fig. 9. Time series plot of electron concentration.

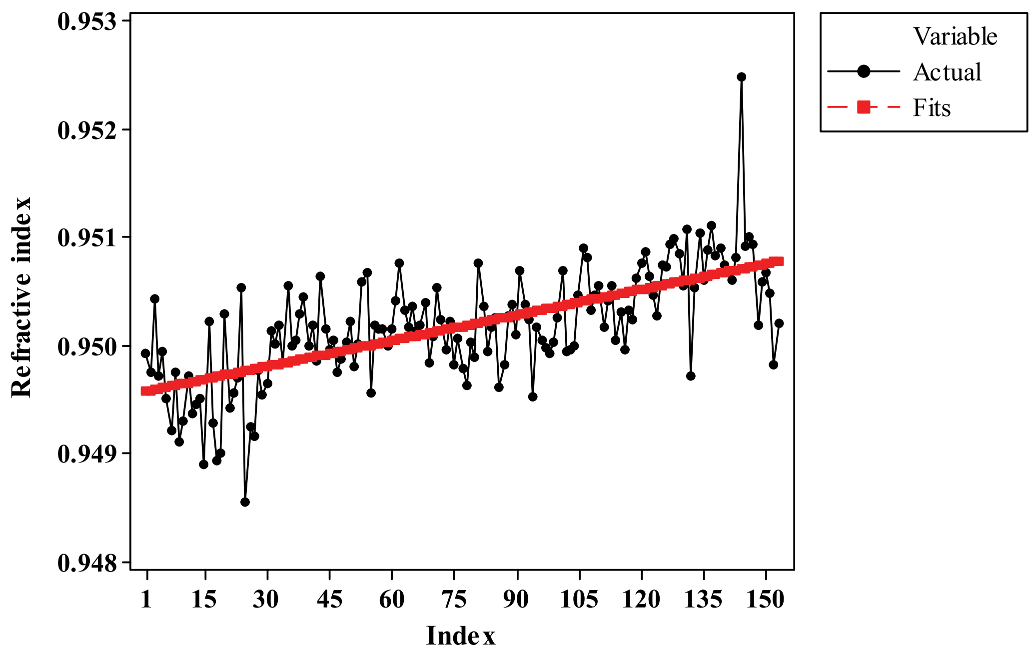

Fig. 10. Time series plot of refractive index.

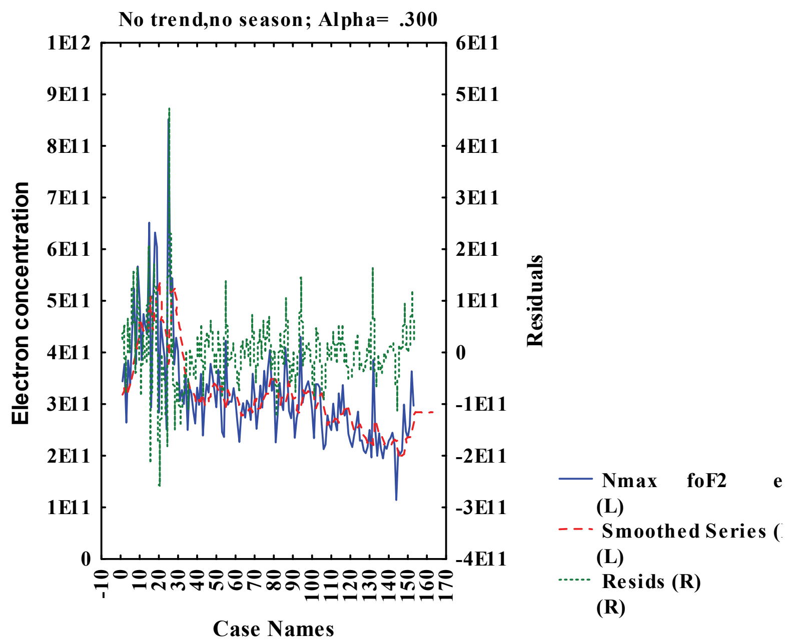

Fig. 11. Electron concentration-actual and exponential smoothing values.

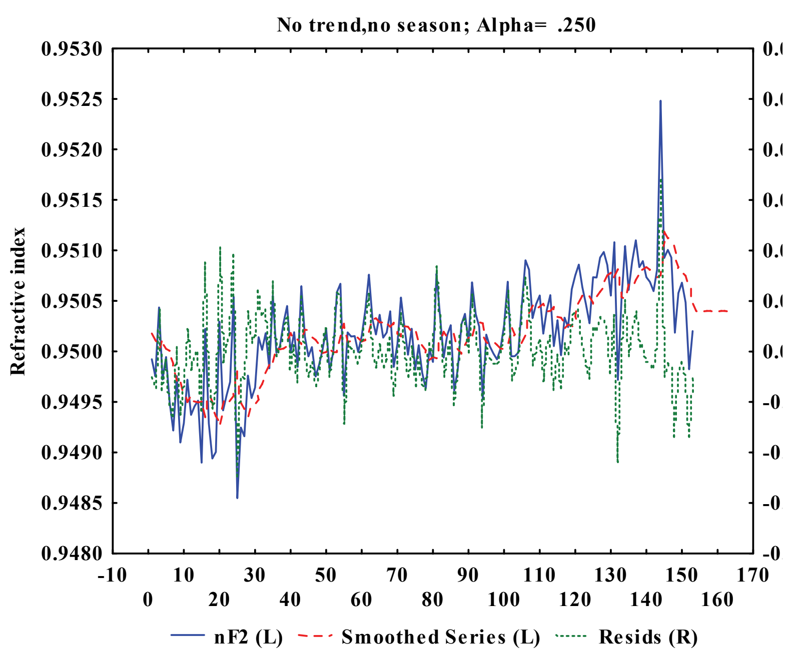

Fig. 12. Refractive index-actual and exponential smoothing values.

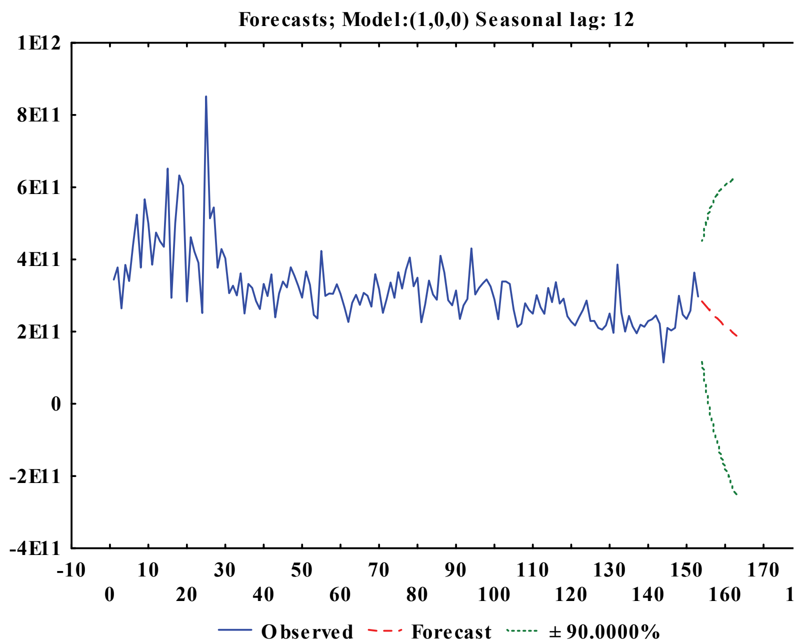

Fig. 13. Forecasting graph of electron concentration.

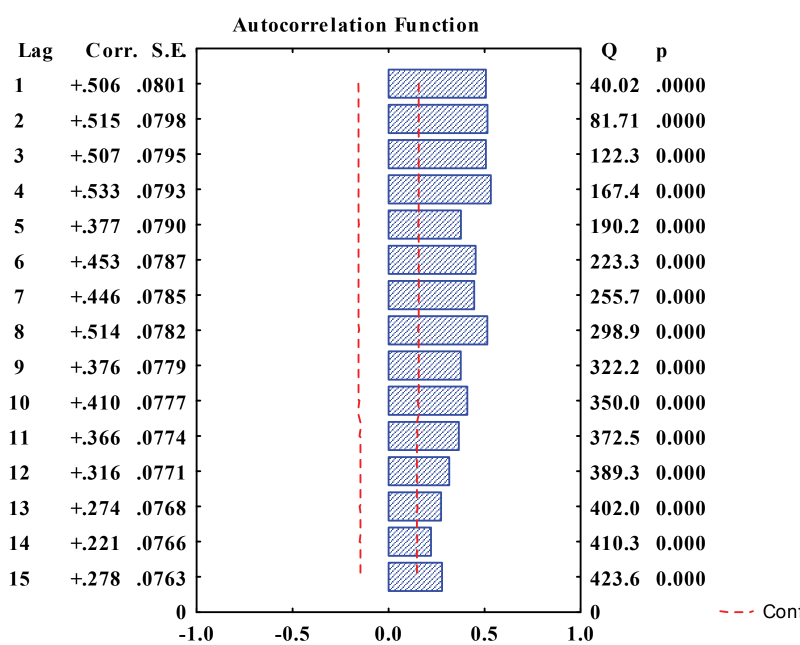

Fig. 14. Illustration of autocorrelation function for TEC.

ARIMA models to handle time-correlated modeling and forecasting. A general ARIMA (p,d,q) model defines autoregressive order, difference and moving average respectively. Autoregressive process is a stochastic difference equation, a mathematical model in which the current value of a series is linearly related to its past values, plus an additive stochastic shock [9&10]. To estimate the impact of solar radiation on TEC and refractive index of F_2 layer at day time and F layer in night, an autoregressive of order one {AR (1)} general model as given in expression (16). A developed stochastic model for ionosphere layer is used to estimate the TEC and refractive index over Islamabad ionosphere region.

$$X_t = \varphi_t X_{t-1} + \varepsilon_t \tag{16}$$

ε_t: Source of randomness and is called white noise.

φ_t: Autoregressive Coefficient

The general model AR (1,0,0), for TEC, the estimates of autoregressive parameters is 0.95556, the standard error 0.02470, the value of t-statistic 38.68 of 153 and lower-95% confidence, upper-95% confidence are 0.906767 and 1.004361 for probability < 0.05. In case of refractive index autoregressive parameter is 0.999950 where the standard error is zero, see Table 3.

Table 3. Parametric description of F_2 layer.

Variable	TEC- P(1)	n – P(1)
Coefficient	0.95556	0.99995
Std Err.	0.02470	0.00
t-statistics	38.680	-
P	0.00	-
Low 95% Confidence	0.906767	-
Up 95% Confidence	1.004361	-

4.6 Forecasting

In the time series of Figs. 9 & 10 follow a repeating pattern, X_t is highly correlated with $X_{t-cycle}$. To create time series model such that the error between the predicted value of the variable and the actual value is as small as possible. The model use lag values of the TEC are used as predictor variables. The TEC forecast value is calculated using Eq-(16), $X_t = 0.95556*2.8376*10^{11} + 0.0247 = 2.71149*10^{11}$ also mentioned in Table 4. The time series for total electron density forecast is presented in Fig. 13.

Table 4. Forecast values of TEC of F_2 layer.

	Forecast
154	2.837691E+11
155	2.711596E+11
156	2.591103E+11
157	2.475965E+11
158	2.365944E+11
159	2.260811E+11
160	2.160350E+11
161	2.064353E+11
162	1.972621E+11
163	1.884966E+11

An autocorrelation is the correlation between the target variable, TEC and lag values for the TEC. Correlation values range from -1 to +1 show that the two variables move together perfectly. In the presentation the estimated correlation between i^{th} observation and the $(i + m)^{th}$ observation on Y-axis vs the lag number on the X-axis [8]. On examining autocorrelation illustrated in Fig. 14 the highest autocorrelation is + 0.533 which occurs with a lag 4. Hence we desire to be sure to include lag values up to 4 when building the model. The second column of the autocorrelation indicates the standard error of the autocorrelation. The autocorrelation bars indicates positive significant autocorrelations occurred for lags 1 to 15. The statistical significance (Q statistical) is mentioned on the right hand side.

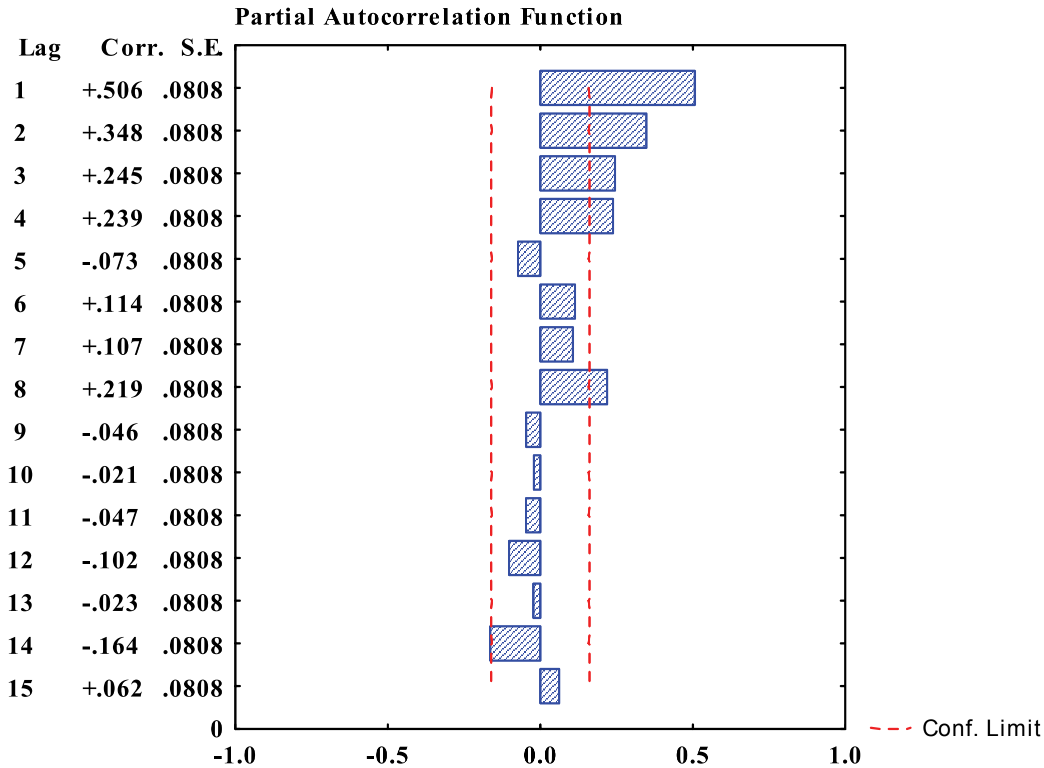

Fig. 15. Partial autocorrelation function for TEC.

The partial autocorrelation is the autocorrelation of time series observations separated by a lag of k time units with the effects of the intervening observations disqualified [9]. The partial autocorrelation plot is shown in Fig. 15 present statistical significance for 1 to 4, 8 and all other lags are 95% confidence interval bands.

5. RESULTS AND CONCLUSION

The presence of ionosphere and change in its characteristics with time is a potential source of radio wave communication. This communication has described physical behavior of ionosphere at Pakistan upper atmosphere region. The result of the processing of radio sounding data determines the statistical values mentioned in Tables 1 to 4 for realization of varying ion concentration and radio refractivity during day and night for long distance communication via ionosphere. The trends and the data pattern variability are also visible in graphical representations and discussed under relevant sub headings.

The Exploratory Data Analysis carried out and the models have been developed, has provided a comprehensive statistical description of the process. It is concluded that methodology adapted is suitable in a sense that only input required are the measured values of critical frequency and altitude for the F_2 layer. It is witnessed that the main advantage of this method is its simplicity. The computed values of parameters are found reasonably accurate. It is seen that the ARIMA (1) is found suitable for predicting and finding forecast for ionosphere parameter under study. The variability in ionosphere electron concentration (N) resulted in varying refractive index (n) and its effect on the long distance communication has been observed in this study.

6. ACKNOWLEDGEMENTS

The authors are grateful to the officials of Pakistan Space & Upper Atmosphere Research Commission (SUPARCO) for provision of ionosphere data. The data helped us in carrying out this research work and producing this publication. This work enables the effective radio communication with respect to the radio wave bending.

7. REFERENCES

1. Barclay, L. *Propagation of Radio Waves*, *2nd ed*. The Institution of Electrical Engineers, London, United Kingdom (2003).
2. Dolukhanov, M. & B. Kuznetsov. *Propagation of Radio Waves*, translated by Boris Kuznetsov. Mir Publishers, Moscow (1971).
3. Schunk, R.W. & A.F. Nagy. *Ionospheres Physics, Plasma Physics, and Chemistry*. Cambridge University Press, Cambridge, UK (2004).
4. Rishbeth, H. & O.K. Garriott. *Introduction to Ionospheric Physics.* Academic Press, Library of Congress, 5th Avenue, New York 10003, USA (1969).
5. Arora, P.N. & S. Arora. *Comprehensive Statistical Methods*, *1st ed*. New Delhi, India (2007).
6. Murphy, A.H. & R.W. Katz. *Probability, Statistics, and Decision making in the Atmospheric Sciences*. Westview Press, USA (1985).
7. Spyros Makridakis, S; C. Steven; W. Wright & V. E. Mcgee, *Forecasting: Methods and Applications*, *2nd ed.* John Wiley & Sons, New York, USA (1983).
8. Francis X.D. *Elements of Forecasting*. South-Western College Publishing, Ohio, USA (1998).
9. Shumway, R.H. & D.S. Stoffer. *Time Series Analysis and Its Applications with R Examples*, 2nd ed. Springer Private Limited, India (2008).
10. Francis, F.C. *Introduction to Plasma Physics*. Plenum Press, New York, USA (1974).
11. Georg Kennedy, G. & B. Davis, *Electronic Communication Systems*, *4th ed*. McGraw Hill, International ed. Electrical Engineering Series, Singapore (1993).
12. George E.P. B; G.M. Jenkins & G.C. Reinsel. *Time Series Analysis, Forecasting & Control*, *3rd ed.* Dorling Kindersley, India (2004).
13. Toti, S.H.C.; A.G.W. Steyn & R.H. Stumpf. *Graphical Exploratory Data Analysis*. Springer-Verlag New York Berlin Heidlberg (1986).
14. Sizun, H. *Radio Wave Propagation for Telecommunication Applications*. Springer New York, USA (2005).
15. Ayubzai M.Y. & S.A. Nazeer. *Wavelet Characterization of Computed Faraday Rotation due to the Interaction of Radio Wave with Ionospheric Plasma*, 10th International Pure Mathematics Conference on Statistical Science (ICCS-X), August 19-21, Quaid-i-Azam University, Islamabad, Pakistan (2009).
16. Ayubzai M.Y. & S.A. Nazeer. *Wavelet Analysis of the Interaction of Radio Waves with Ionospheric Plasma at Pakistan's Upper Atmosphere*, International Conference on Frontiers of Physics (ICFP 2009), Tribhuan University, Kathmandu, Nepal (2009).
17. Ayubzai M.Y. & S.A. Nazeer. Study the effect of fluctuating dynamics of ionospheric plasma on radio wave communication. *Journal of Astrophysics and Applied Mathematics* 1: 141-150 (2009).